RESEARCH ARTICLE

TIME-LAPSE POROSITY AND VELOCITY ANALYSIS USING ROCK PHYSICS MODELS IN NIGER DELTA, NIGERIA

Emmanuel Aniwetalu, Akudo Ernest, Juliet Ilechukwu, Okechukwu Ikegwuonu, Uzochukwu Omoja

[a] Department of Applied Geophysics Nnamdi Azikwe University, Awka Anambra State.
[b] Department of Geology, Federal University, Lokoja, Kogi State.
[c] Department of Geology Chukwuemeka Odumegwu Ojukwu University, Uli Anambra State
[d] Department of physics, Nnamdi Azikwe University, Awka Anambra State
* Corresponding Author's Email: eu.aniwetalu@unizik.edu.ng

ARTICLE DETAILS

ABSTRACT

The analysis of 3-D and time-lapse seismic data in Isomu Field has offered the dynamic characterization of the reservoir changes. The changes were analyzed using fluid substitution and seismic velocity models. The results of the initial porosity of the reservoirs was 29.50% with water saturation value of12%.The oil and gas maintained saturation values of 40% and 48% with average compressional and shear wave velocities of 2905m/s and 1634m/s respectfully. However, in fluid substitution modelling, the results reflect a change in fluid properties where average gas and oil saturation assume a new status of 34% and 24% which indicates a decrease by 14% and 16% respectively. The average water saturation increases by 30% with an average value of 42%. The decrease in hydrocarbon saturation and increase in formation water influence the porosity. Thus, porosity decreased by 4.16% which probably arose from the closure of the aspect ratio crack due to pressure increase.

KEYWORDS

Niger Delta, Reservoir monitoring, Porosity, Velocity and Seismic Data

1. INTRODUCTION

An objective approach to porosity modeling and velocity depth imaging has been a subject of contention among geophysicists. This argument is led by two notable schools of thought, namely, those who believe that true depth imaging is not possible and will never be possible and those who hold on to a contrary view. However, all arguments may have their places, but in recent times, the subsurface porosity and velocity modeling system have offered a solution for improved depth imaging, reservoir monitoring, and management. This has attracted the interest of geoscientists who also recognized the importance of velocity in placing constraints on subsurface variations in lithology, porosity, and pore-fluid content (Stewart et al., 2003). However, compressional and shear (S) wave velocities are controlled by different elastic properties and their ratio (Vp/Vs) have been greatly used in the science of rock physics which link geophysical observations and the physical properties of rocks.

Fundamentally, the seismic wave is elastic energy that travels within the earth whose precise velocity depends on the rock types. For instance, compressional waves travel through all types of materials including solids, liquids, and gases. Shear waves travel through solids but not through liquids and gases because the shear modulus of a fluid is close to zero (Gregory, 1976). Consequently, the shear wave velocity (Vs) is not sensitive to variations in pore fluid content as compressional velocity (Vp). Compressional velocity may travel through all materials within the earth,

but using it alone for depth modeling and interpretation is ambiguous, but the inclusion of shear wave data and modeling can significantly reduce the ambiguity associated with interpreting seismic data (Shillington et al., 2008). This signifies that compressional and shear wave velocities are important properties for improved local seismic event location and seismic hazard studies (Afegbua et al., 2016).

Although determining their precise values and modeling of their variations in siliciclastic sediment is a serious challenge because of production-induced changes in the reservoirs which may affect the reservoir geometries and consequently, impact on reservoir fluid saturation, pressure, porosity, and compressibility properties (Hermansen et al., 2000; Gambolati and Teatini, 2015). Generally, hydrocarbon production is associated with pore pressure, fluid saturation, temperature, and porosity changes in the reservoir and these have profound effects on seismic elastic properties in a variety of ways, such that changes in elastic reservoir properties over a time-lapse are considered a function of changes in pore pressure and water saturation. Therefore, using rock-physics models, these pore-filled fluid properties and their effects on porosity and velocity at the in-situ condition of the reservoir was modeled from the primary well logs.

The time-lapse porosity and velocity logs were derived from these primary logs using forward modeling and integrated with time-lapse seismic data to monitor the changes in reservoir properties. The objective among others is to monitor porosity and velocity changes arising from

hydrocarbon production in the reservoirs using well logs and time-lapse seismic data which has recently gained more popularity in imaging the effects of fluid flow in a producing reservoir (Fanchi, 2001; Landrø, 2001; Pendrel, 2006; Lumely 2001). The influence of fluid saturation on elastic properties of rocks in porous media depends on pore geometry, fluid-phase distribution, pressure, and saturation. This has been the subject of many theoretical and experimental investigations (Gassman, 1951; Biot, 1956; Wang, 1997; Wylie et al., 1956, Geertsma 1961, Domenico, 1977; Murphy, 1984).

2. GEOLOGIC BACKGROUND

The study area is located in Isomu Field in the coastal swamp depobelt of the western Niger Delta (Figure 1). The Niger Delta basin ranks among the world's most prolific provinces of hydrocarbons and its geology has been discussed by several authors (Weber et al., 1987; Evamy et al., 1978; Doust and Omatsola, 1990). Reijers stated that the productivity of the basin depends on its strata package formed from a major regressive cycle that resulted in the deposition of allocyclic units of transgressive marine sand; marine shale, shoreface, and fluvial (Reijers, 2011). Cretaceous strata were first described by where three major lithostratigraphic units were identified (Short and Stauble, 1967). They are (a) the prodelta facies (Akata Formation), (b) the paralic delta front facies (Agbada Formation), and (c) the continental facies (Benin Formation). The Akata Formation is the oldest of the three formations and serves as the source of rock with ages ranging from Eocene to Recent (Reijers et al., 1997; Short and Stauble 1967). The Agbada Formation is a hydrocarbon-bearing unit consisting mainly of sandstones and intercalation of shales (Okeugo et al., 2018). The Benin Formation is the youngest and comprises the top part of the Niger Delta clastic wedge, from the Benin–Onitsha area in the north to beyond the coastline (Short and Stauble, 1967).

3. MATERIALS AND METHODS OF DATA ANALYSIS

The material used in this study includes suites of well logs, well tops, and check shot data that provides velocity information required to calibrate the well log with seismic reflection, 3D and time-lapse (4D) seismic data acquired at different vintages in Isomu Field in western Niger Delta, Nigeria. It is one of the brown fields whose wells have continued to record a decline in production. The well log data consists of gamma-ray log, density log, compressional, and shear wave slowness. The 3-D seismic data surveys covered about 175kms². The 3-D seismic data set was acquired in the late nineteen eighties (1980s).

In July 2012, a 3D reshoot/4D repeat acquisition was completed over the field. As part of the time-lapse processing, a subset of a repeated survey and the legacy survey were processed through amplitude-preserving processing for reservoir monitoring purposes. However, the differences resulting from the acquisition design, noise and other non-production related variations were minimized between the two seismic surveys in a process known as cross-equalization. The focus is to enhance the repeatability of the surveys and reduce random data variations while preserving and enhancing the presence of production-related changes. The basic geometric parameter used for 3-D and Time-Lapse seismic data acquisition in the field is shown in Table 1.

3.1 Calibration of Well Log to Seismic Data

In well to seismic data correlation, a check shot data was used to adjusts the sonic log velocities or the log time-depth curve to match the time-depth relationship obtain from seismic data. Using this information, well logs in-depth domain was scaled with seismic data by converting well log depth to time using E-LOG program. Statistical wavelet extraction was carried out on the seismic data, basically to estimate the filter that best fit the well log reflection coefficients to the input seismic data at the well locations (Figure 2a). The seismic wavelet is in zero phase distance from the well with a sampling rate of 2ms. The wavelet length and taper length are 200 and 25ms respectively. The extracted wavelet was applied to the original log to generate zero offset synthetic traces where stretch and squeeze operations were carried out on synthetic traces to enhance the results as shown in Figure 2b.
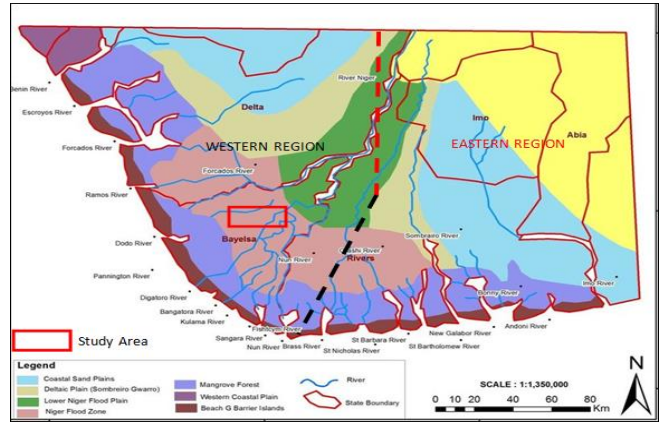

Figure 1: Map of Niger Delta showing the study area.

Table 1: Geometry of 3D (Base) and 4D (Monitor) Seismic Survey of Isomu Field.

| Geometry type	Swath (off end) 3D Seismic survey	Swath (off end) 4D Seismic survey
Bin size	25m× 25m (conventional)	25m × 25m (conventional)
Receiver lines	6	6
Receiver line spacing	350m	350m
Total active channels	960 channels	80 × 6 = 480 channels
Active channel per line	160 channels	80
Receiver spacing	50m	50m
Source line spacing	500m	500m
Source points per salvo	14m (either side of active spread)	7m
Source spacing	50m	50m
Inline rolling	500m (one source line)	500m (one source line)
Cross line rolling	350m (one receiver line)	350m (one receiver line)
Maximum offset	4484m	2865m
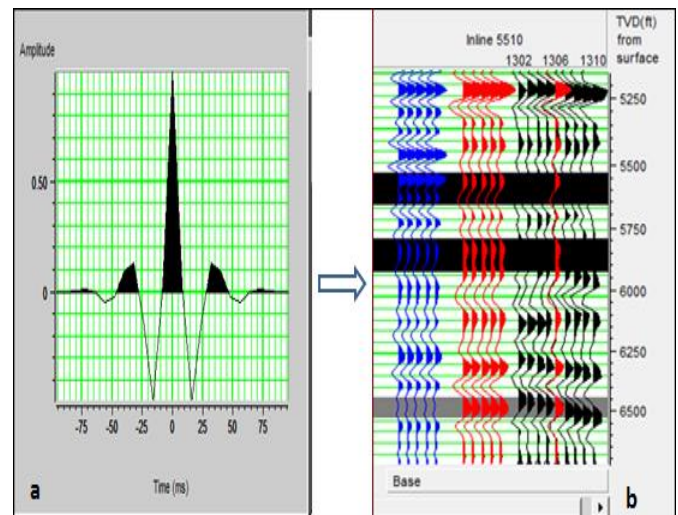
Figure 2: (a) Statistical wavelet time response and (b) seismic to well ties.

3.2 Timelapse Velocity and Porosity Modelling

In velocity modeling, compressional and shear wave slowness at chosen depth intervals were estimated using the information provided by the P-wave and shear wave logs (Figure 3). For instance, at the depth interval of 6600ft, the values of compressional and shear wave slowness were estimated as 9500ft/s and 3250ft/s respectfully. The compressional and shear wave slowness (feet per second) were transformed into compressional (Vp) and shear wave velocities (meters per second) using equations 1 and 2, respectively.

$$Vp = \Delta tp \times 0.305 \tag{1}$$

$$Vs = \Delta ts \times 0.305 \tag{2}$$

Where Vp, Vs, Δtp, and Δts is the compressional velocity, shear wave velocity, the interval transit time recorded by compressional log, and shear sonic log respectfully.

Similarly, density and gamma-ray values at the depth were directly estimated from the well logs but in-situ porosity values were calculated simply by transforming the observed density data at the corresponding depths into standard porosity measurements using equation 3.

$$\phi = \frac{\rho_{ma} - \rho_b}{\rho_b - \rho_f} \tag{3}$$

Where φ is porosity, ρ_{ma} is the density of rock matrix, taken to be 2,650kg/m³, ρ_b = observed bulk density recorded by density tool, and ρ_f = Density of fluid, taken to be 1,080 kg/m³.
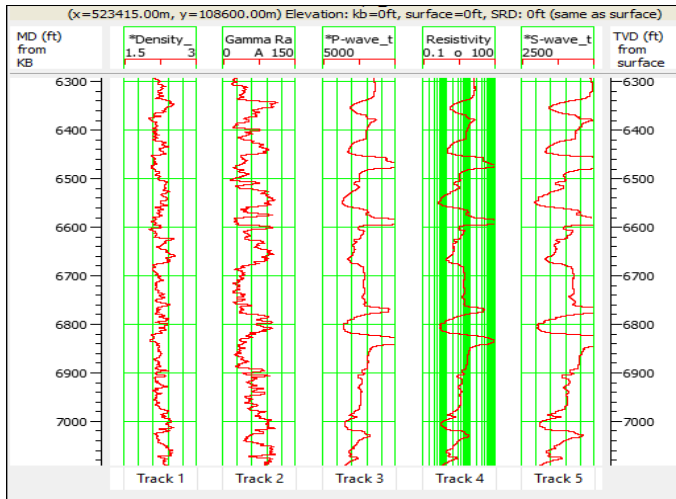

Figure 3: Isomu_1 showing Gamma ray log, Density log, Compressional and shear velocity logs

The modeled porosity logs were cross-plotted with log-derived velocity to obtain the porosity depth profile. This represents the predevelopment porosity values of the formation. However, to understand the changes in reservoir porosity with stages of production, forward modeling of the original logs were performed using the Biot-Gassmann equation. The equation relates the bulk modulus of a saturated rock (Ku), to the dry rock bulk modulus (Kd), the solid grain modulus (Ks), the fluid bulk modulus (Kf), and the porosity φ as shown in equation 4.

$$Ku = Kd + \frac{(1 - Kd/Ks)^2}{\frac{\phi}{Kf} + 1 - \frac{\phi}{Ks} - \frac{Kd}{Kd2}} \tag{4}$$

Therefore, using E-LOG program, we specify the input logs as P-wave, S-wave, and density. The analysis windows were defined using tops. We assumed that input density is known and porosity was set to be calculated. Similarly, for S-wave, we assumed that Castagna's equation is correct for wet case. Therefore, to perform fluid replacement modeling on the wells, we present three fluid scenarios such as water, gas and oil.. However, the petrophysical parameters were specified using matrix and fluid property calculator. The oil and gas properties were calculated using FLAG 2014 Global Oil Model and FLAG 2014 global respectively. The calculation includes the bubble point effect which was carried out using the standing equation of the bubble point method (BPM). In matrix property calculation, density, bulk, and shear modulus of the rock minerals present in the reservoir were calculated using the Hashin-Shrikman average. In fluid property calculation, the menu calculated the density, bulk modulus, and fluid saturations using the information obtained from the PVT data and inferred post-production data (Table 2). These pore-filled fluid properties represent the in-situ condition that was used to calculate effective elastic moduli and bulk densities using theoretical models. These were applied and the new P-wave, S-wave, and density logs that predict changes in the elastic properties of the reservoir as a result of changes in fluid content were generated. The new time-lapse porosity log was calculated from the density. Furthermore, the time-lapse logs were

integrated with 4-D seismic data to create a depth domain profile of the time-lapse seismic velocity model. However, using sample interval of 8ms in seismic volume, we specify the domain type (depth), range of the output model and create a depth domain horizon in seismic data. Using the model filtering option after interpolation, we applied a smoother model trace in the output domain with the high cut frequency (10/15Hz,) and the velocity depth models were created. The slices of velocity depth maps were extracted from the velocity depth models and possible production-related changes were mapped.

Table 2: Fluid Parameters and their initial Values used in FRM

S/n	Parameters	Initial Values
1	Temperature	70deg C 158 deg F 343.15 K
2	Pressure	2900.65 Psi
3	Oil GOR	100 L/L 561.5 scf/bbl
4	Gas gravity	0.6
5	Water Salinity	15000ppm
6	Water Saturation	12%
7	Hydrocarbon Saturation	88%

4. RESULTS AND DISCUSSIONS

The sensitivity of porosity and velocity to changes in reservoirs fluid properties arising from hydrocarbon production has been examined using rock physics models. The porosity, gamma-ray, density, compressional, and shear wave velocity values computed from the well logs (Table 3). The zones under consideration are between 5800ft and 8100ft with six distinct reservoirs grouped as HD1000, HD2000, HD2600, HD3000, and HD5000. These zones consist of a vast total rock volume characterized by a thick sand sequence with little non-reservoir characteristics. The average porosity value of the reservoir is 29.50% with a very low water saturation of 12%. The oil and gas drive has average saturation of 40% and 48% respectively. A very low water saturation complements a very high hydrocarbon saturation value of 88%. The average compressional and shear velocities are 2905m/s and 1634m/s respectfully. The in-situ condition of the temperature, pressure and salinity content is 70deg, 2900psi, and 1500ppm respectively. As evident in table 2 and table 3, porosity varies with depth, low and high porosity values also complement high and low-velocity values respectfully. The cross-plot relation and cross-sections between the porosity and velocity are shown in Figure 4a-b. The cross plot results indicate a clear relationship between velocities and porosities (Figure 4b). The results show variation in velocity and porosity with depth where velocity increases with decrease in porosity.

Table 3: The in-situ log readings at selected depth points in Isomu-1

Depth (ft)	Vp (ft/s)	Vp (m/s)	Vs (ft/s)	Vs (m/s)	Gamma Ray (API)	Density (g/cc)	Porosity %
6600	9500	2898	3250	991	105	2.25	0.3101
6680	8750	2669	3259	994	45	2.10	0.3400
6740	11000	3355	6875	2097	45	2.40	0.2600
6760	11750	3584	6250	1906	60	2.47	0.2711
7000	8000	2440	4000	1220`	40	2.10	0.3521
7020	9500	2898	4600	1403	65	2.22	0.3312
7060	12500	3813	6925	2112	68	2.40	0.2511
7080	9350	2852	4000	1220	45	2.10	0.2922
7100	11441	3489	6301	1921	75	2.40	0.2851
7120	9023	2752	4523	1379	50	2.20	0.3232
7140	9027	2753	4528	1381	45	2.21	0.3281
7180	10349	3156	5672	1729	50	2.31	0.3013
7200	10480	3196	5891	1796	55	2.32	0.2922
7300	10823	3301	5973	1822	60	2.34	0.2825
7400	9782	2983	4910	1498	45	2.21	0.3218
7500	10960	3343	5782	1764	62	2.28	0.2715
7800	11139	3397	6236	1902	90	2.44	0.2516
8000	11432	3486	6431	1961	91	2.45	0.2503
8100	10991	3352	6000	1830	70	2.31	0.2729

The identification of the prospect also involves the observation made to identify velocity and porosity response that can be related to hydrocarbon presence in the reservoirs. The crossplot of velocity and porosity color coded with porosity shows good separation between sand and shale and

between brine and oil sand. A very low value of porosity and a very high value of velocity are defined by shale lithology as indicated in the red color overlay of the cross plot. However, high value of porosity and low value of velocity defined the sand lithology as indicated by blue (hydrocarbon) and green (brine) color overlay. These zones are characterized by hydrocarbon and brine saturation as indicated in the reservoirs defined by the tops.
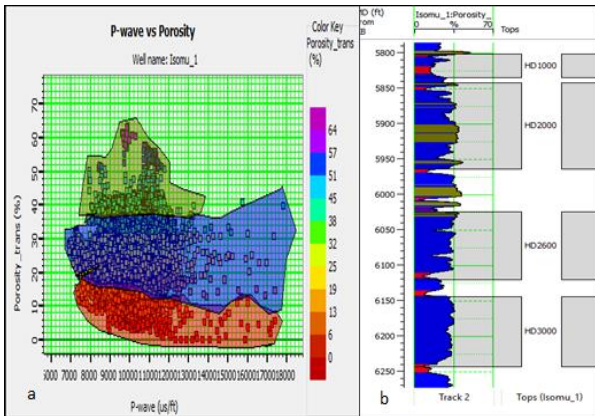

Figure 4: (a) The cross plot of porosity versus velocity and (b) cross-section of the porosity in the Isomu_1.

Although, the porosity and velocity decrimination of the fluids and lithology with depth is not continous because velocity exhibits different behavior in different porosity domains. For a very high porosity rocks, the velocity is not strongly dependent on the suspension domain (critical porosity) where solid particles are suspended in the fluid but changes in the consolidated rock domain (below critical porosity) especially for relatively low porosity rocks. However, the changes in porosity and velocity to fluid saturation and pressure in the reservoirs were effectively discriminated in fluid substitution modeling. Here, complex combination of forces acting on the reservoirs as production progresses were determined. These forces may be gravitational, chemical, and mechanical in origin which are the geological and geophysical processes that occur in the reservoirs undergoing hydrocarbon production. Details of these changes are shown in the output model of the P-wave, S-wave velocity, density, and time-lapse porosity logs (Figure 5). The log curves reflect the changes in the fluid properties in the substitution zone.

For gas, oil and water drive, there are significant changes in time-lapse fluid saturation and pressure which probably arise from production related effects. The average gas and oil saturation is 34% and 24% respectively which indicates a decrease in gas and oil saturation by 14% and 16% respectively. The histogram plot of water saturation shows the range of water distribution with an average value of 42% which also indicates an increase by 30% relative to 12% of the connate water (Figure 6). The decrease in hydrocarbon saturation and increase in water drive is an indication of reservoir depletion because water aquifer is in hydraulic communication with the hydrocarbon reservoir especially for a reservoir that has natural water drives. The void spaces left behind as hydrocarbon production progress are replaced with water. These are production-related changes that affect the surrounding rock geometry and the internal flow areas such as connecting pores or permeability. However, in theses pore spaces, the difference between the wellbore pressure and the average reservoir pore fluid pressure represents the flow driving force responsible for the reduction of porosity of reservoir rock with the increase in pressure (Figure 7a).

The force that may control the fluid flow in the internal flow areas of reservoir is the difference between the overburden stress and the average reservoir pore fluid pressure. However, the time-lapse porosity (porosity at new fluid conditions) decreases by 4.16% which probably arises from the closure of the aspect ratio crack. The porosity change influences the elastic moduli of the rocks, pressure, transport properties, and velocity in different scales. The compressional wave velocity increases with an increase in pressure because of the progressive crack closure. Hence, in the new fluid conditions, compressional velocity increases with an average velocity of 12689ft/s (Figure 7b). Furthermore, the effects of the fluid properties on the velocity at varying temperature and pressure in the

reservoirs were simulated and the results show that oil and gas velocity increases with an increase in pressure (Figure 8a-b).
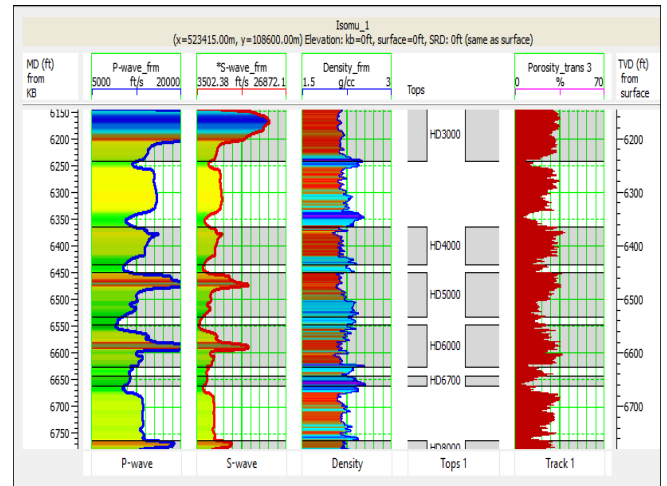

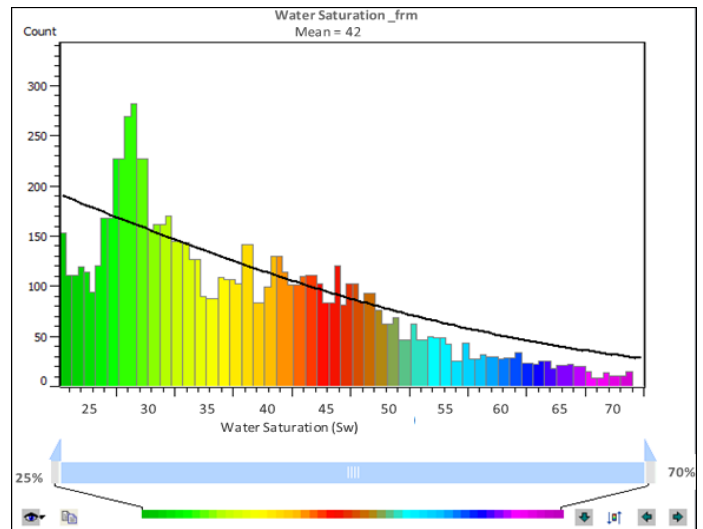**Figure 5:** The well log response to fluid replacement modelling

Figure 6: The histogram plot of time-lapse water saturation
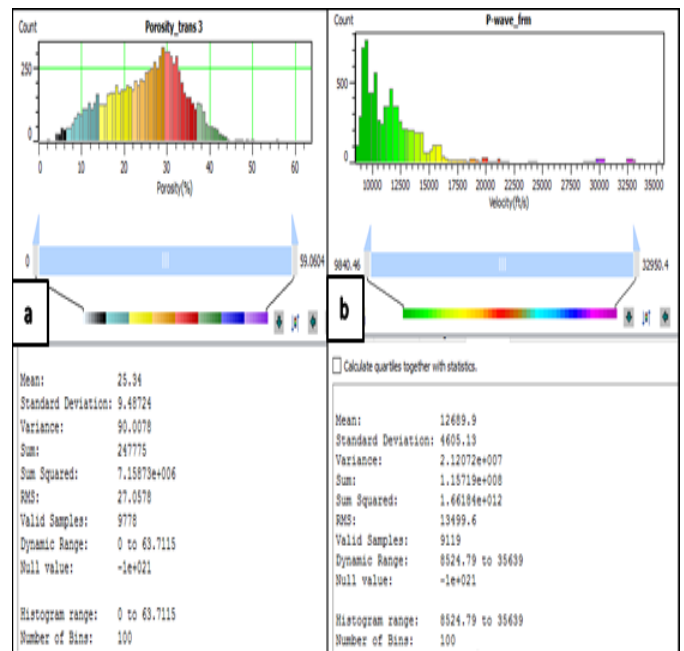

Figure 7: (a) The histogram plot of time-lapse porosity; (b) Compressional wave velocity.

The oil velocity maintained constant velocity at 2000Psi but decreases with an increase in temperature (Figure 8c). Gas velocity decreases with an increase in temperature at a very low-temperature range of about 1-40degF but increases with an increase in temperature from 40degF (Figure 8d). Similarly, oil modulus increases linearly with an increase in

pressure and decreases with an increase in temperature (Pendrel, 2006). Gas modulus increases with an increase in pressure. However, pressure does not affect brine modulus and brine density. The pressure and temperature effects on these velocities are enhanced with dissolved gas. Oil with dissolved gas maintained a low velocity, density, and modulus when compared to the oil without dissolved gas on GOR.

However, the effects of these new fluid conditions in the reservoirs (HD2000) were also evident in the velocity depth model of the base and monitor seismic data (Figure 9a-b). In the depth model of the base, velocity is very low especially at the well locations which are an indication of hydrocarbon charged sand (Landro and Stammerjer, 2004). The relatively high velocity in the central part of the slice is an indication of connate water (blue color code) and formation pressure (pink color code). However, in the velocity depth model of the monitor, the reservoir shows a significant increase in velocity that probably arises from an increase in water saturation and pore pressure. The anomalous increase in velocity in the monitor as a result of water replacing hydrocarbon in the reservoir is an indication of reservoir depletion.
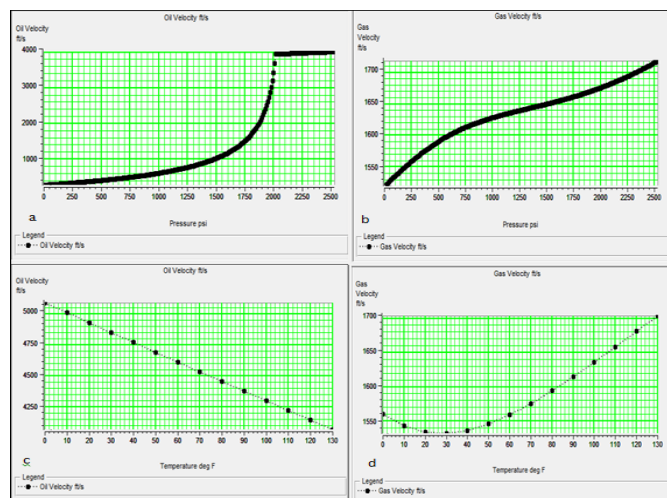

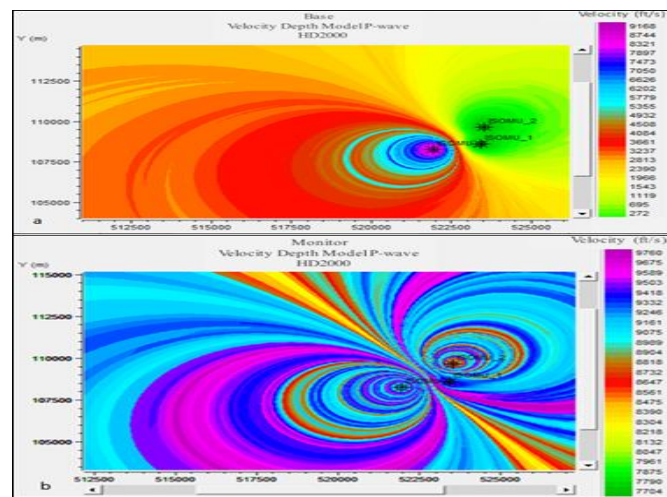**Figure 8:** Effects of fluid properties on velocity under temperature and pressure

Figure 12: (a) Velocity depth model base at HD2000; (b) monitor at HD2000

5. CONCLUSION

Effect of production-related changes on velocity and porosity in the Coastal Swamp depobelt of the Niger Delta have been examined using well logs and velocity depth models of the base and monitored seismic data acquired at different vintages. The objective, among others, is to model the porosity and velocity changes arising from hydrocarbon production in the reservoir. The results showed significant changes in fluid properties which affect in-situ porosity and velocity. The average gas and oil saturation is 34% and 24% respectively which indicates a decrease in gas and oil saturation by 14% and 16% respectively. The water saturation increase by 30% relative to 12% of the connate water. The decrease in hydrocarbon

saturation and increase in water saturation is an indication of reservoir depletion.

The reservoir depletion is accompanied by an increase in pore pressure which gives rise to the closure of the aspect ratio crack. In these new fluid conditions, porosity decreases by 4.16% and also affects the elastic moduli of the rocks, transport properties, and velocity However, velocity increases with an increase in pressure and decreases with an increase in porosity. The effects of the fluid properties on the velocity at varying temperature and pressure in the reservoir show that velocity, density, and modulus of oils increase with increasing pressure and decrease with increasing temperature. The behavior of the fluid properties on velocity was also analyzed using the velocity depth model of 3-D and 4-D seismic data acquired at different vintages. The results similarly showed an increase in velocity in almost all well locations in the depth model to monitor. This probably results from production-related effects such as increasing water saturation and pore pressure that normally occur during hydrocarbon production. However, the major shortcoming in this study is our inability to quantify the remaining hydrocarbon volume in the depleting reservoirs. Therefore, the future research should concentrate on this direction

REFERENCES

Afegbua, K.U., Ezomo, F.O., 2013. Evaluation of the performance of Z-component of Nigerian Seismographic stations from spectral analysis. International Journal of Physical Sciences, 8 (11), Pp. 428-442.

Biot, M.A., 1956. Theory of propagation of elastic waves in fluid-saturated porous solids. II. Higher frequency range. J. Acoust. Soc. Am., 28, Pp.179–191.

Domenico, S.N., 1977. Elastic properties of unconsolidated porous sand reservoirs. Geophysics, 42, Pp. 1339.

Doust, H., Omatsola, E., 1990. Niger Delta, in, Edwards, J.D., and Santogrossi, P.A., eds., Divergent/ Passive Margin Basins, AAPG memoir 48: Tulsa, American Association of petroleum geologists, Pp. 239-248.

Evamy, B.D., Haremboure, J., Kamerling, P., Knaap, W.A., Molloy, F.A., Rowlands, P.H., 1978. Hydrocarbon habitat of Tertiary Niger Delta: American Association of Petroleum Geologists Bulletin, 62, Pp. 277-298.

Fanchi, J.R., 2003. Estimating Geomechanically Properties Using an Integrated Flow Model. Pp. 108-116.

Gambolati, G.I., Teatini, P.O., 2015. Geomechanics of subsurface water withdrawal and injection. Water Resources research, 51 (6), Pp. 3922-3955.

Gassmann, F., 1951. Elastic Waves through a Packing of Spheres. Geophysics, Pp. 673- 685.

Geertsma, J., Smit, D.C., 1961. Some aspects of elastic wave propagation in fluid-saturated porous solids. Geophysics, 26, Pp. 169-181.

Gregory, A.R., 1976. Fluid saturation effects on dynamic elastic properties of sedimentary rocks. Geophysics, 41, Pp. 895-92 1.

Hermansen, B.A., Sylte, J.E., and Thomas, L.K., 2000. Reservoir characterization of Ekofisk Field: a giant,fractured chalk reservoir in the Norwegian North Sea-history match. SPE Reservoir Evaluation and Engineering, 3 (06), Pp. 534-543.

Landro, M., and Stammeijer, J., 2004. Quantitative estimation of the compaction and velocity Changes using 4D impedance and travel time changes, Geophysics, 69 (4), Society of Exploration Geophysicist.

Lumley, D.E., 2001. Time-lapse seismic reservoir monitoring. Geophysics, 66, Pp. 50–53.

Murphy, W.F., Winkler, K.W., and Kleinberg, R.L., 1985. Acoustic relaxation in sedimentary rocks. Dependence on grain contacts and fluid saturation, Geophysics, 51 (3), Pp. 757-766.

Okeugo, C.G., Onuoha, K.M., Ekwe, A.C., and Dim, C.I., 2017. Rock quality Prediction Using Cross plots and Seismic lithology Inversion: An example of XIN Field, Eastern Niger Delta Basin. AAPG Annual Convention and Exhibition.

Pendrel, J., 2006. Seismic inversion- A critical tool in reservoir characterization: Scandinavian Oil-gas magazine, Pp. 19-22.

Reijers, T.A., 2011. Stratigraphy and sedimentology of the Niger Delta. Geologos, 17 (3), Pp. 133–162.

Reijers, T.J.A., Petters, S.W., and Nwajide, C.S., 1997. The Niger Delta Basin,In: R.C. Selley, (ed.). Africa Basins – Sedimentary Basin of the World 3: Amsterdam, Elsevier Science, Pp. 151-172.

Shillington, D.J., Timothy, A.M., Christine, P.A., and John, M.O., 2008. P- and S-wave velocities of consolidated sediments from a seafloor seismic survey in the North Celtic Sea Basin, offshore Ireland.

Short, K.C., and Stauble, A.J., 1967. Outline of Geology of Niger Delta. AAPG Bull., 51, Pp. 761-779.

Stewart, R.R., Gaiser, J.E., Brown, R.J., and Lawton, D.C., 2003. Converted-wave seismic exploration. Applications. Geophysics, 68, Pp. 40–57.

Wang, Z., 1997. Feasibility of time-lapse seismic reservoir monitoring: The physical basis: The Leading Edge, 16, Pp. 1327–1329.

Weber, K.J., 1987. Hydrocarbon distribution patterns in Nigerian growth fault structures controlled by structural style and stratigraphy: Journal of Petroleum Science and Engineering, 1, Pp. 91-104.

Wyllie, M.R.J., Gregory, A.R., and Gardner, L.W., 1956. Elastic wave velocities in Heterogeneous and porous media. Geophysics, 21, Pp. 41-70